Available online at www.sciencedirect.com
SCIENCE DIRECT®
Scripta Materialia 53 (2005) 1123–1128
Scripta MATERIALIA
www.actamat-journals.com

Crystal structure and electrochemical characteristics of $La_{0.9}Mg_{0.1}Ni_{5-x}Sn_x$ ($x = 0.1$, 0.2, 0.3, 0.4) alloy electrodes

Xinbo Zhang [a], Danzi Sun [b], Wenya Yin [a], Yujun Chai [a], Minshou Zhao [a,*]

[a] *Key Laboratory of Rare Earth Chemistry and Physics, Changchun Institute of Applied Chemistry, Graduate School of Chinese Academy of Sciences, No. 5625 Renming Street, Changchun 130022, PR China*
[b] *State Key Laboratory of Electroanalytical Chemistry, Changchun Institute of Applied Chemistry, Graduate School of Chinese Academy of Sciences, Changchun 130022, PR China*

Received 14 November 2004; received in revised form 28 April 2005; accepted 25 July 2005
Available online 22 August 2005

Abstract

The crystal structure and electrochemical performance of $La_{0.9}Mg_{0.1}Ni_{5-x}Sn_x$ ($x = 0$–0.4) system compounds have been investigated systematically. It is found that the addition of Sn is beneficial to the dischargeability of the alloy electrodes at low temperature but detrimental to the dischargeability at high temperature. Moreover, addition of Sn is beneficial to both charge retention and high rate dischargeability.

Keywords: Metal hydride electrode; Charge efficiency; Discharge efficiency; High rate chargeability; High rate dischargeability

1. Introduction

The nickel–metal hydride (Ni–MH) secondary battery has been widely adopted in many fields by virtue of its many advantages: high power density, high resistance to overcharging and overdischarging, capability of performing a high rate charge/discharge, environmental friendliness and interchangeability with nickel–cadmium battery [1–4]. As the most important component in a Ni–MH battery, metal hydride electrodes have attracted significant attention during the last decade [5–8]. However, in order to compete favorably with some other secondary batteries, alloys with higher energy density, faster activation and lower cost are urgently required. Recently, Kadir et al. [9–12] have reported that R–Mg–Ni based alloys can absorb–desorb 1.8–1.87 mass% H_2, and are therefore regarded as promising candidates for reversible gas hydrogen storage. As to their electrochemical hydrogen storage, Kohno et al. [13] developed several kinds of La–Mg–Ni–Co hydrogen storage electrodes and showed that the discharge of $La_{0.7}Mg_{0.3}Ni_{2.8}Co_{0.5}$ alloys reaches 410 mAh g^{-1}. Unfortunately, the La–Mg–Ni–Co system hydrogen storage electrode alloys have some disadvantages, such as a high absorption/desorption plateau pressure, and poor cyclic stability. Pan et al. [14] have systematically studied the structure and electrochemical properties of $La_{0.7}Mg_{0.3}(Ni_{0.85}Co_{0.15})x$ ($x = 3.0$–5.0) alloys and pointed out that $La_{0.7}Mg_{0.3}(Ni_{0.85}Co_{0.15})_{3.5}$ suffers the poorest cyclic stability although it has the highest discharge capacity among the alloy electrodes. It is well known that elemental substitution is one of the most effective methods for improving the overall properties of the hydrogen storage alloys and obtaining the desired overall properties, e.g. proper capacity at a favorable hydrogen pressure, favorable high rate dischargeability (HRD) and good cyclic stability [15–18]. Liu et al. [19]

* Corresponding author. Tel.: +86 431 5262365; fax: +86 431 5685653.
E-mail address: eboat@ciac.jl.cn (M. Zhao).

1359-6462/$ - see front matter © 2005 Acta Materialia Inc. Published by Elsevier Ltd. All rights reserved.
doi:10.1016/j.scriptamat.2005.07.035

indicated that Co substitution for Ni can obviously improve the cyclic durability of the later charge/discharge cycles of the La–Mg–Ni–Mn–Co system alloy electrodes, while the discharge capacity decay of the starting charge/discharge cycles cannot be effectively prevented. Moreover, the existence of Co in these alloy electrodes increases the price greatly, making it unfavorable for practical applications. Lambert et al. [20] reported that tin substituted compounds have especially attractive properties because they show no line broadening and little capacity decay even after 10,000 cycles. It was found that Sn substitution for Ni in $LaNi_5$ alloy electrodes results in an obvious improvement of discharge capacity and cycle life of the alloy electrodes and improves the kinetics of hydrogen absorption–desorption [21]. Furthermore, Luo et al. [22] observed that the use of Sn as a partial substitute for Ni in $LaNi_5$ leads to a significant decrease in the hysteresis ratio. As to their electrochemical characteristics, Deng et al. [23] indicated that substitution of tin for Ni in $LaNi_5$ can apparently improve the electrochemical performance of the alloys.

With regard to the criteria of high discharge capacity and low cost of raw materials, in the present study the influence of partial substitution for Ni with Sn on the structural and electrochemical properties of the $La_{0.9}Mg_{0.1}Ni_{5-x}Sn_x$ ($x = 0.1$, 0.2, 0.3, 0.4) hydrogen storage alloys were studied in order to improve the overall properties of the La–Mg–Ni system alloy.

2. Experimental details

2.1. Alloy preparation, X-ray diffraction

All samples were prepared by arc melting the constituent metals or master alloy on a water-cooled copper hearth under an argon atmosphere. The purity of all the metals, i.e., La, Mg, Ni, and Sn, was higher than 99.9 mass%. A slight excess of Mg over stoichiometric composition was needed in order to compensate for evaporative loss of Mg during synthesis. Several attempts were made until the optimum preparative conditions were found. The alloys were turned over and remelted five times to ensure good homogeneity. The weight loss of the alloys was less than 1 mass% during melting. Therefore, no chemical analyses were carried out. Thereafter, the alloy samples were crushed in a mortar and pestle into fine powders of −300 mesh size.

Crystallographic characteristics of the hydrogen storage alloys were investigated using a Rigaku D/Max 2500PC X-ray diffractometer (CuK_α radiation, Bragg–Brentano geometry, 2θ range 20–110°, step size 0.02°, backscattered rear graphite monochromator). The lattice constants and cell volume were calculated by a cell program [24] after internal theta calibration using silicon as standard reference materials.

2.2. Electrochemical measurements

The preparation of the disk-type electrodes, the setup of the electrochemical cell and the measurement of electrochemical properties were similar to those described in our previous paper [25]. The charge efficiency was obtained according to Senoh's previous paper [26]. Both the HRD and the linear polarization curves of the alloy electrodes were measured according to our previous paper [27].

The charge retention (CR) of the negative electrode could be evaluated using the following equation [28]

$$\mathrm{CR} = \{1 - 2C_2/(C_1 + C_3)\} \times 100/\mathrm{day}\ (\%\mathrm{day})$$

where C_1 represented the discharge capacity measured after the activation (by repeated charge–discharge cycling), C_2 was the discharge capacity measured after the storage on open-circuit conditions for a given period of time, and C_3, the discharge capacity measured in the charge–discharge cycle immediately after the measurement of C_2.

3. Results and discussion

3.1. Structure characteristic

Fig. 1 shows XRD patterns of $La_{0.9}Mg_{0.1}Ni_{5-x}Sn_x$ ($x = 0.1$, 0.2, 0.3, 0.4) alloys synthesized by arc melting. The sharp diffraction peaks indicate a long-range crystallographic order and excellent crystallinity of the alloy. It can be found that all the alloys have single $CaCu_5$-type phase. Careful examination of the diffraction angle reveals some slight shifts between these patterns, which depend on Sn content in the alloys. The lattice parameter, cell volume and density of the alloys are listed in Table 1. It can be clearly seen that both the lattice

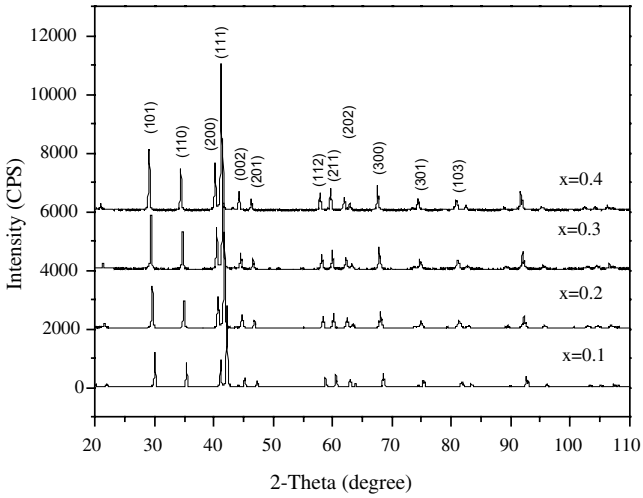

Fig. 1. XRD patterns of $La_{0.9}Mg_{0.1}Ni_{5-x}Sn_x$ ($x = 0.1$, 0.2, 0.3, 0.4).

Table 1
Lattice parameters, cell volume and densities of $La_{0.9}Mg_{0.1}Ni_{5-x}Sn_x$ ($x = 0.1, 0.2, 0.3, 0.4$)

Sn-stoichiometry	Lattice parameter		Cell volume ($Å^3$)	Density ($g\,cm^{-3}$)
	a (Å)	c (Å)		
0.1	5.019	3.981	86.86	7.8449
0.2	5.025	3.986	87.16	8.0445
0.3	5.031	3.995	87.57	8.2318
0.4	5.049	4.001	88.34	8.3832

parameters and the cell volumes monotonically increase with increasing x value in the alloys, which is mainly ascribed to the fact that the atomic radius of Sn (1.405 Å) is larger than that of Ni (1.246 Å).

3.2. Discharge capacity and cycling stability

The curves of the discharge capacity vs. the cycle number at 298 K for the $La_{0.9}Mg_{0.1}Ni_{5-x}Sn_x$ ($x = 0.1$, 0.2, 0.3, 0.4) alloy electrodes are shown in Fig. 2. It can be seen that all the alloy electrodes can be activated to reach their maximum capacity within four cycles, which means that activation of the alloy electrodes is easy. With the increase of x, the maximum discharge capacity of the alloy electrode increases first from 254.6 mAh g^{-1} ($x = 0.1$) to 295.3 mAh g^{-1} ($x = 0.3$) and then decreases to 283.8 mAh g^{-1} ($x = 0.4$). This is an indication of the occurrence of two opposing factors that contribute to the specific capacity of the alloy electrodes. On the one hand, as the atomic radius and atom volume of Sn are larger than those of Ni, the addition of Sn will result in a larger cell volume of the alloys, as shown in Table 1, and thus increase the interstitial positions of the lattice cell, which will be beneficial to the specific capacity of the alloy electrodes. On the other hand, as the atomic weight of Sn (118.69) is also greater than that of Ni (58.67), the mole masses of these compounds increase with increasing x and thus the number of lattice cells per unit mass of alloy becomes less. This reduces the number of hydrogen-storage units, which is detrimental to the hydrogen-storage capacity. Overall, the combined effect of the two opposite factors mentioned above will thereby result in an optimal value for the Sn content in the alloys. From our work, the recommended amount of Sn addition is 0.3. Moreover, it can be easily found that all the alloy electrodes can still discharge more than 75% of their maximum discharge capacity even after 28 charge–discharge cycles, which is much better than that of the $La_{0.7}Mg_{0.3}Ni_{3.4-x}Mn_{0.1}Co_x$ ($x = 0$–1.6) alloy electrodes in Liu et al.'s paper [19], indicating that the increase in the Sn content in the alloys results in a noticeable improvement of the cyclic stability. There are two major factors that govern the effect of the Sn substitution for Ni on the electrochemical cycling stability of the alloy electrodes. On the one hand, as Bowman et al. [29] points out, Sn addition leads to a smaller change of unit cell on hydriding and hence less pulverization and improvement in the cycling life of the alloy electrodes. On the other hand, Sn can form a dense and strong SnO_2 oxide film on the alloy surface in the alkaline electrolyte, which effectively inhibits further oxidation of the alloy and slows down the corrosion rate of Mg and La and thereby improves the cyclic stability of the alloy electrodes.

3.3. The effect of temperature on charge efficiency

The influence of temperature on the charge efficiency of the $La_{0.9}Mg_{0.1}Ni_{5-x}Sn_x$ ($x = 0.1$, 0.2, 0.3, 0.4) alloy electrode is given in Fig. 3. It can be found that all the alloy electrodes show their maximum charge efficiency at room temperature (298 K) and then decrease with either increasing or decreasing temperature. In particular, when the temperature is lower than 253 K, the charge efficiency pronouncedly decreased to a value even lower than that at 333 K. These results inevitably influence the electrochemical capacity of the alloy at low or high temperature.

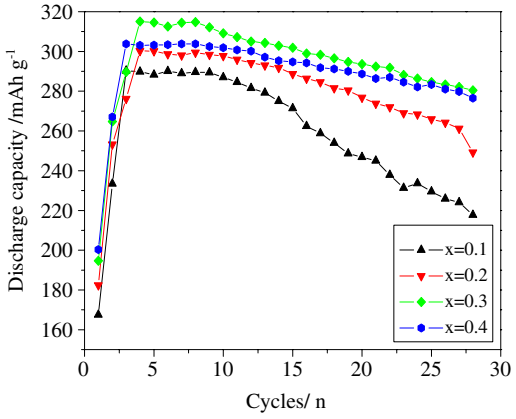

Fig. 2. Discharge capacity vs. cycle number curves for $La_{0.9}Mg_{0.1}Ni_{5-x}Sn_x$ ($x = 0.1$, 0.2, 0.3, 0.4) alloy electrodes at 298 K.

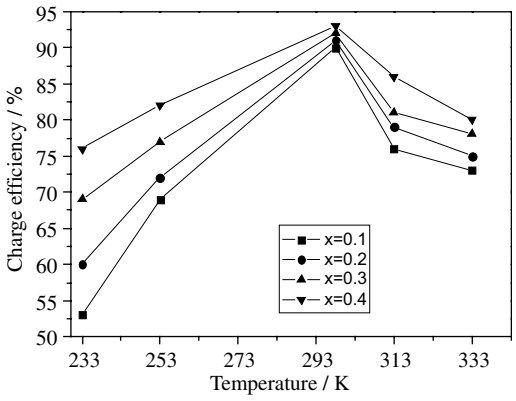

Fig. 3. Charge efficiency for $La_{0.9}Mg_{0.1}Ni_{5-x}Sn_x$ ($x = 0.1$, 0.2, 0.3, 0.4) alloy electrodes as a function of temperature at 60 mA g^{-1}.

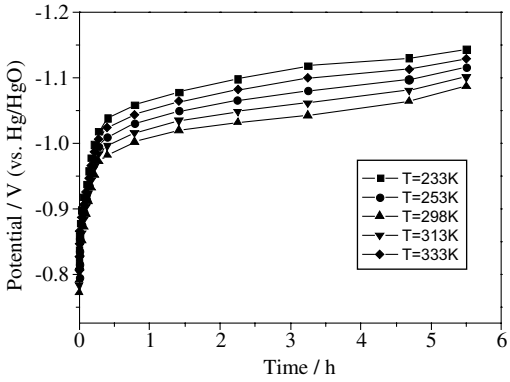

Fig. 4. Charge curves of the $La_{0.9}Mg_{0.1}Ni_{4.7}Sn_{0.3}$ alloy electrodes at different temperatures.

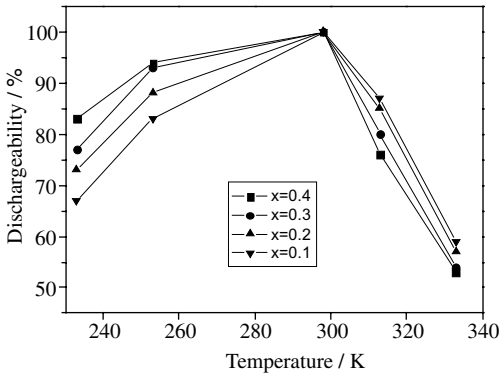

Fig. 5. The dependence of dischargeability on temperature for $La_{0.9}Mg_{0.1}Ni_{5-x}Sn_x$ ($x = 0.1$, 0.2, 0.3, 0.4) alloy electrodes.

In order to find the reason for the phenomenon mentioned above, the charge plateau potential should be considered. Fig. 4 illustrates the charge curves of the $La_{0.9}Mg_{0.1}Ni_{4.7}Sn_{0.3}$ alloy electrode as a representative example of $La_{0.9}Mg_{0.1}Ni_{5-x}Sn_x$ ($x = 0.1$, 0.2, 0.3, 0.4) alloy electrodes at various temperatures. The midpoint potentials are −1.118 V, −1.08 V, −1.04 V, −1.06 V and −1.09 V (vs. Hg/HgO) at 233 K, 253 K, 298 K, 313 K and 333 K, respectively, indicating that the overpotential which is the main determining factor for the charge potential [30] is very sensitive to temperature. That the overpotential of the alloy electrodes varies with temperature perhaps can be explained as follows. On the one hand, it is generally known that the diffusion of hydrogen from bulk to the reaction surface, the electrochemical catalytic activity of the alloy and the conductance of the electrolyte decrease with decreasing temperature, and thereafter concentration polarization, electrochemical polarization and ohmic polarization become serious, which inevitably result in the increase of the overpotential. On the other hand, because the hydride formation is an exothermic reaction, high temperature is detrimental to the charge process. So the serious polarization at low temperature and high temperature would be responsible for decreasing the charge efficiency of the alloy electrodes.

3.4. The dependence of dischargeability on temperature

Negative electrode material used in Ni–MH battery should be capable of working over a wide temperature range. Fig. 5 shows the dischargeability of the $La_{0.9}Mg_{0.1}Ni_{5-x}Sn_x$ ($x = 0.1$, 0.2, 0.3, 0.4) electrodes at different temperatures. It can be easily seen that the dischargeability is very sensitive to temperature. The alloy electrodes reach their maximum discharge capacities at room temperature (298 K) and then decrease sharply with the decrease or increase of temperature. All the alloy electrodes can only discharge less than 60% of their maximum capacity at high temperature (333 K), indicating that they all suffer poor dischargeablity at high temperature, whereas the dischargeabilities of the alloy electrodes at low temperature are quite different. Moreover, we can find that Sn addition is beneficial to the dischargeability of the alloy electrode at low temperature. It is generally known that hydrogen can easily diffuse in the alloys' bulk with large lattice parameter and cell volume, and thus will greatly improve the dischargeability at low temperature because it is hydrogen diffusion control reaction [31]. However, hydrogen evolution also became easier during discharge at high temperature with the increase of the lattice parameter and cell volume of the alloy electrodes, which inevitably decrease the dischargeability of the alloy electrodes at high temperature.

3.5. Charge retention property

Iwakura has pointed out that self-discharge can be divided into two parts: reversible (C_3–C_2), and irreversible (C_1–C_3) ones [24]. The CR values of the $La_{0.9}Mg_{0.1}Ni_{5-x}Sn_x$ ($x = 0.1$, 0.2, 0.3, 0.4) electrodes after seven days are summarized in Table 2. It can be seen that both the reversible and irreversible all decrease with increasing x in the alloys and therefore the self-discharge rate is depressed, indicating that Sn addition is beneficial to the charge retention of the alloy electrodes. It is known that Sn addition enlarges the cell volume of the alloy electrodes and thus decreases the hydrogen pressure in the alloy electrodes, which is beneficial to decrease the reversible ones. Moreover, Sn addition can decrease the pulverization of the alloy, which accordingly suppresses the deterioration of the hydrogen-absorbing alloy, and thus restrains the irreversible ones.

3.6. High rate chargeability and high rate dischargeability

High rate chargeability (HRC) and HRD are both important kinetic properties for the metal hydride electrode. The influence of charge current density on

Table 2
Summary of the self-discharge data for $La_{0.9}Mg_{0.1}Ni_{5-x}Sn_x$ ($x = 0.1, 0.2, 0.3, 0.4$) alloys

Sn-stoichiometry	C_1 (mAh g^{-1})	C_2 (mAh g^{-1})	C_3 (mAh g^{-1})	C_3–C_2 (mAh g^{-1})	C_1–C_3 (mAh g^{-1})	Self-discharge rate (%day)
0.1	290.3	165.7	258.4	92.7	31.9	5.66
0.2	300.3	183	271.3	88.3	27	5.14
0.3	315.1	199.5	287.2	81.7	25	4.82
0.4	303.8	202.8	279.1	76.3	24.7	4.35

the HRC of the $La_{0.9}Mg_{0.1}Ni_{4.7}Sn_{0.3}$ alloy electrode at various temperatures is shown in Fig. 6. It can be seen that the HRC monotonically decreases with the increasing charge current density in all cases. In particular, at temperatures less than 253 K the charge efficiency decreases obviously. Iwakura et al. [32] pointed out that the HRC of alloy electrodes is mainly controlled by the electrochemical formation reactions of atomic hydrogen on the electrode surface and/or the succeeding hydrogen diffusion in the alloy bulk. Moreover, it is generally known that the hydride formation is an exothermic reaction. Higher temperature is beneficial to former two sides and lower temperature is favorable to the third one. The combined effect of the above factors results in an optimal temperature for HRC of the alloy electrodes. In the present study, the alloy electrode shows its best HRC at 298 K.

Fig. 7 shows the HRD for $La_{0.9}Mg_{0.1}Ni_{5-x}Sn_x$ ($x = 0.1$–0.4) alloy electrodes as a function of discharge current densities. As can be seen from this figure, the HRD of all the alloy electrodes decrease with increasing discharge current density, and thus results in the decreasing of the discharge capacity of the alloy electrodes. For a discharge current density of 1200 mA g^{-1}, the HRD and the discharge capacity of the alloy electrodes are shown in Table 3. It can be easily found that the HRD value is significantly increased by the addition of Sn. It is generally accepted that the high rate dischargeability of a metal hydride electrode is mainly determined by the charge-transfer process occurring at the metal electrolyte interface and/or the hydrogen diffusion process in the hydride bulk [32,33]. To examine the

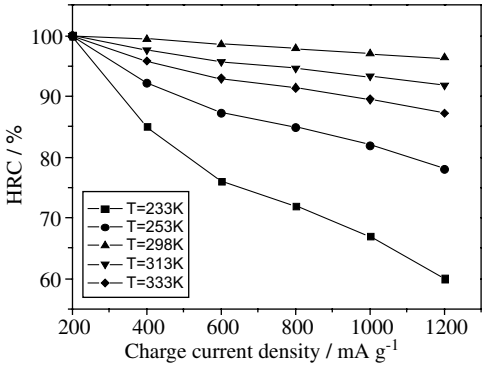

Fig. 6. High rate chargeability (HRC) of $La_{0.9}Mg_{0.1}Ni_{4.7}Sn_{0.3}$ alloy electrode at different temperatures as a function of charge current density.

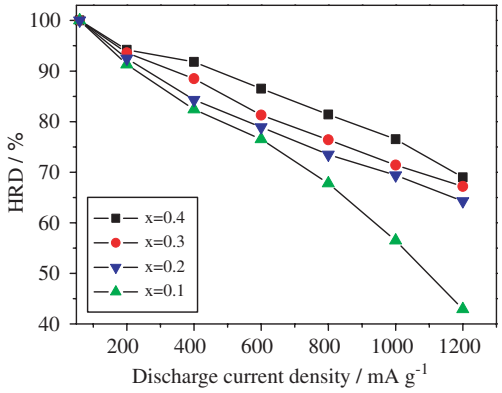

Fig. 7. HRD as a function of discharge current density for $La_{0.9}Mg_{0.1}Ni_{5-x}Sn_x$ ($x = 0.1, 0.2, 0.3, 0.4$) alloy electrodes at 298 K.

Table 3
The electrochemical kinetic parameters of $La_{0.9}Mg_{0.1}Ni_{5-x}Sn_x$ ($x = 0.1, 0.2, 0.3, 0.4$) alloy electrodes

Samples	HRD_{1200}[a] (%)	Discharge capacity (mAh g^{-1})[a]	Polarization resistance[b] R_p (mΩ)	Exchange current density[b] I_0 (mA g^{-1})
$x = 0.1$	42.9	124.5	179.02	143.3
$x = 0.2$	64.3	193.1	113.79	225.6
$x = 0.3$	67.2	211.7	107.47	239.1
$x = 0.4$	69	209.6	103.91	247.1

[a] The high rate dischargeability at the discharge current density of 1200 mA g^{-1}.
[b] Calculated at 298 K.

effect of the partial substitution of Sn for Ni on the HRD, linear polarization is performed on these alloy electrodes. Based on the measured linear polarization curves, values of exchange current density I_0 and polarization resistance R_p was evaluated for the alloy electrodes and are summarized in Table 3. It can be seen that the polarization resistance R_p of the alloy electrodes decreases with increasing x, accordingly the exchange current density I_0 of the alloy electrodes increases from 143.3 to 247.1 mA g^{-1} when x increases from 0.1 to 0.4. The variation of I_0 value with the HRD_{1200} of the alloy electrodes is shown in Fig. 8. The high rate dischargeability shows a linear relationship with the exchange density I_0 for the alloy electrodes with $x =$ 0.1–0.4. Iwakura et al. [33] have pointed out that if the electrochemical reaction on the surface is the rate-determining factor, a linear dependence of the high rate

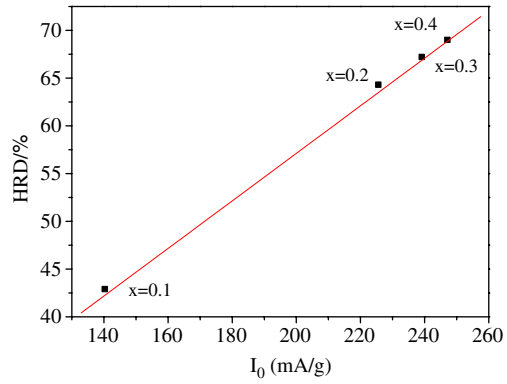

Fig. 8. High rate dischargeability (HRD) at 1200 mA g^{-1} as a function of exchange current density (I_0) for $La_{0.9}Mg_{0.1}Ni_{5-x}Sn_x$ alloys ($x = 0.1$–0.4).

dischargeability on the exchange current density should be observed. In contrast, if the diffusion of hydrogen in the bulk is the rate-determining factor, the high rate chargeability/dischargeability should be constant, irrespective of exchange density. Therefore, in the present study, the HRD is essentially controlled by the charge-transfer reaction of hydrogen on the surface at a discharge current density of 1200 mAh g^{-1}.

4. Conclusion

X-ray powder diffraction studies of the $La_{0.9}Mg_{0.1}Ni_{5-x}Sn_x$ ($x = 0.1$, 0.2, 0.3, 0.4) system compounds >reveal that the addition of Sn changes the lattice parameter, cell volume and density without changing the crystal structure of the fundamental $LaNi_5$ structure (P6/mmm, $CaCu_5$ type). The results show that $La_{0.9}Mg_{0.1}Ni_{4.7}Sn_{0.3}$ has the highest discharge capacity (295.3 mAh g^{-1}) among the alloys studied. It is found that Sn addition is beneficial to the dischargeability for the alloy electrode at low temperature but detrimental to the dischargeability at high temperature. Moreover, Sn addition is beneficial to both the improvement of the charge retention characteristics and the high rate dischargeability. In the present study, the HRD is essentially controlled by the charge-transfer reaction of hydrogen on the surface at a discharge current density of 1200 mAh g^{-1}.

Acknowledgment

This work was financially supported by the National Natural Science Foundation of China (grant no. 20171042).

References

[1] Iwakura C, Matsuoka M. Prog Batteries Battery Mater 1991;10:81.
[2] Sakai T, Miyamura H, Kuriyama N, Kato A, Oguro K, Ishikawa H. J Electrochem Soc 1990;137:795.
[3] Willems JJG. Philips J Res 1984;39(1):1.
[4] Wang CS, Lei YQ, Wang QD. Electrochim Acta 1998;43:3193.
[5] Oesterreicher H, Clinton J, Bittner H. Mater Res Bull 1974;11:2282.
[6] Oesterreicher H, Ensslen K, Kerlin A, Bucher E. Mater Res Bull 1980;15:275.
[7] Takeshita T, Wallace WE, Craig RS. Inorg Chem 1974;13:2282.
[8] Bechman CA, Goudy A, Takeshita T, Wallace WE, Craig RS. Inorg Chem 1976;15:2184.
[9] Kadir K, Sakai T, Uahara I. J Alloys Compds 1997;257:115.
[10] Kadir K, Nuriyama N, Sakai T, Uehara I, Eriksson L. J Alloys Compds 1999;284:145.
[11] Kadir K, Sakai T, Uahara I. J Alloys Compds 1999;287:264.
[12] Kadir K, Sakai T, Uahara I. J Alloys Compds 2000;302:112.
[13] Kohno T, Yoshida H, Kawashima F, Inaba T, Sakai I, Yamamoto M, et al. J Alloys Compds 2000;311:L5.
[14] Pan HG, Liu YF, Gao MX, Zhu YF, Lei YQ, Wang QD. J Alloys Compds 2003;351:228.
[15] Wu JM, Li J, Zhang WP, Muo FJ, Tai LC, Xu RG. J Alloys Compds 1997;248:180.
[16] Notten PHL, Latroche M, Percheron-Guegan A. J Electrochem Soc 1999;146(9):3181.
[17] Wallace WE, Pourarlan F. J Phys Chem 1982;86:4958.
[18] Ma JX, Pan HG, Chen CP, Wang QD. J Alloys Compds 2002;343:164.
[19] Liu YF, Pan HG, Gao MX, Li R, Lei YQ. J Alloys Compds 2004;376:304.
[20] Lambert SW, Chandra D, Cathey WN, Lynch FE, Bowman Jr RC. J Alloys Compds 1992;187:113.
[21] Ratnakumar BV, Witham C, Fultz B, Halpert B. J Electrochem Soc 1994;141(8):L89.
[22] Luo S, Clewley JD, Flanagan TB, Bowman Jr RC, Wade LA. J Alloys Compds 1998;267:171.
[23] Deng HX, Zhuang YH, Liu JQ, Guo J, Lu JX, Yan JL. J Alloys Compds 2004;376:211.
[24] Takaki Y, Taniguchand T, Hori K. J Ceram Soc Jpn Int Ed 1993;97:362.
[25] Zhang XB, Chai YJ, Yin WY, Zhao MS. J Solid State Chem 2004;177:2373.
[26] Senoh H, Hara Y, Inoue H, Iwakura C. Electrochim Acta 2001;46:967.
[27] Zhang XB, Sun DZ, Yin WY, Chai YJ, Zhao MS. Electrochim Acta, 50(9), 1957–64.
[28] Iwakura C, Kajiya Y, Yoneyama H, Sakai T, Oguro K, Ishikawa H. J Electrochem Soc 1989;136(5):1351.
[29] Bowman RC, Luo CH, Ahn CC, et al. J Alloys Compds 1995;185:217.
[30] Sakai T, Miyamura H, Kuriyama N, Kato A, Oguro K, Ishikawa H. J Less-Common Met 1990;159:127.
[31] Sakai T, Miyamura H, Kuriyama N, Kato A, Ogura K, Ishikawa H. J Electrochem Soc 1990;137:795.
[32] Iwakura C, Matsuoka M, Asai K, Kohno T. J Power Source 1992;38:335.
[33] Iwakura C, Oura T, Inoue H, Matsuoka M. Electrochim. Acta 1996;41(1):117.